Inverse Design of a Graphene-Based Quantum Transducer via Neuroevolution - Supplemental Information

Kevin Ryczko,[*,†,‡] Pierre Darancet,[*,¶,§] and Isaac Tamblyn[*,‖,†,‡]

†*Department of Physics, University of Ottawa, Ottawa, ON K1N 6N5, Canada*
‡*Vector Institute for Artificial Intelligence, Toronto, OM M5G 1M1, Canada*
¶*Center for Nanoscale Materials, Argonne National Laboratory, Lemont, IL 60439, United States*
§*Northwestern Argonne Institute of Science and Engineering, Evanston, IL 60208, United States*
‖*National Research Council of Canada, Ottawa, ON K1N 5A2, Canada*

E-mail: kevin.ryczko@uottawa.ca; pdarancet@anl.gov; isaac.tamblyn@nrc.ca

A Proof of Principle for Device Optimization

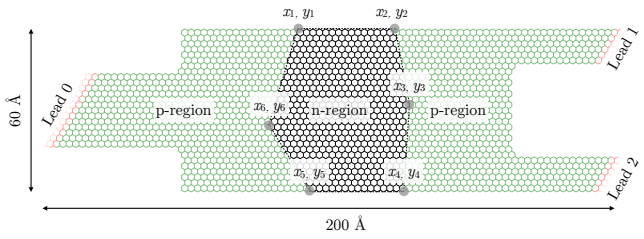

Figure S1: Visual representation of the polygon strategy. The lattice sites that are within a polygon that is drawn with 6 points are declared to be p-doped where everything else is declared to be n-doped.

In what we call our 'polygon strategy' we define a n-doped region by defining a set of 6 points and drawing a convex hull. All other regions of the device are p-doped. Such a device can be seen in Figure S1. The genes of the structure are the set of points that defines the convex hull. The values y_1, y_2, y_4, and y_5 are fixed during the optimization process. The same methodology outlined in the Methods section of the manuscript is applied here, except the set of points are updated rather than the weights of the artificial neural network (ANN) policy:

$$\begin{pmatrix} x_1, y_1 \\ x_2, y_2 \\ \vdots \\ x_6, y_6 \end{pmatrix}_{\text{new}} = \begin{pmatrix} x_1, y_1 \\ x_2, y_2 \\ \vdots \\ x_6, y_6 \end{pmatrix}_{\text{old}} + \alpha \begin{pmatrix} u_{11}, u_{12} \\ u_{21}, u_{22} \\ \vdots \\ u_{61}, u_{62} \end{pmatrix} \tag{1}$$

Following the same protocol as before we ran 64 independent optimizations, each with a different random seed. In each of the optimizations, we track the structure that maximizes the optimization function. In Figure S2 we plot the average, maximum and standard deviation optimization function, purity of valley currents, and valley currents of those devices. Comparing to the results of the ANN policy, we can see that the performance in this strategy is weaker. We obtain an average valley current purity of $\sim 82\%$ for K' and $\sim 78\%$ for K.

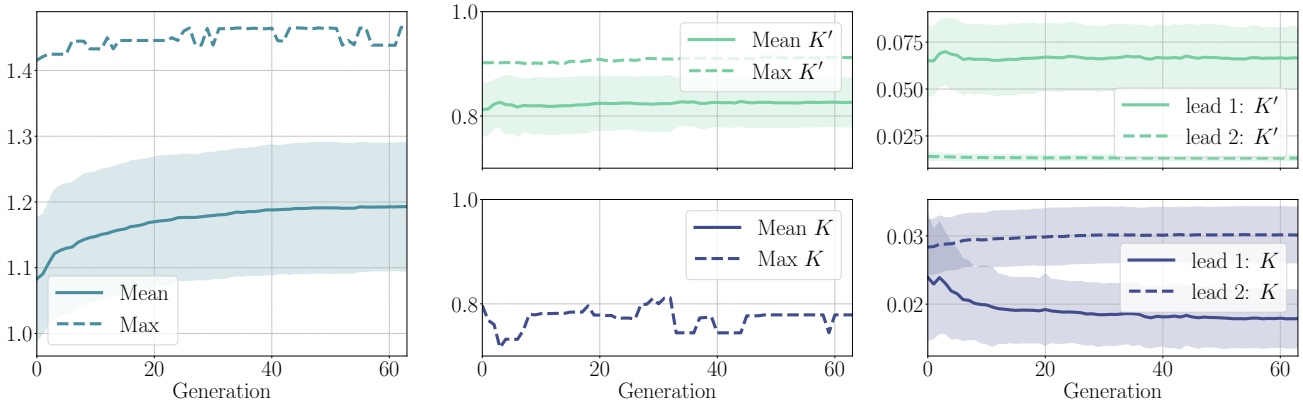

Figure S2: Optimization curves (left), valley current purity (middle), and valley currents (right) recorded during the optimization processes using the polygon policy. For each independent optimization, the devices with the maximum objective functions are recorded. The solid lines show the average values of these devices and the lighter regions show the standard deviations.